IMAGE ENHANCEMENT BY REGION DETECTION ON CFA DATA IMAGES

S. Battiato, S. Cariolo, G. Gallo
D.M.I. – University of Catania - Viale A. Doria 6, 95125, Catania, Italy
battiato@dmi.unict.it, cariolo@dmi.unict.it, gallo@dmi.unict.it

G. Di Blasi
Department of Linguistics, University of Calabria, Ponte Pietro Bucci, Cubo 17b, Rende, Italy
gdiblasi@unical.it

Keywords: Image enhancement, Principal Component Analysis, Expected color rendition.

Abstract: The paper proposes a new method devoted to identify specific semantic regions on CFA (Color Filtering Array) data images representing natural scenes. Making use of collected statistics over a large dataset of high quality natural images, the method uses spatial features and the Principal Component Analysis (PCA) in the HSL and normalized-RG color spaces. The classes considered, taking into account "visual significance", are skin, vegetation, blue sky and sea. Semantic information are obtained on pixel basis leading to meaningful regions although not spatially coherent. Such information is used for automatic color rendition of natural digital images based on adaptive color correction. The overall method outperforms previous results providing reliable information validated by measured and subjective experiments.

1 INTRODUCTION

Usually typical consumer devices acquire image on CFA data format: each input pixel contains a single chromatic channel, according to some specific pattern (e.g. Bayer Pattern [Bayer, 1976]). It has been shown like low-level processing can be effectively performed on CFA domain [Bosco et al, 2002], [Lukac et al, 2004]. In this paper we propose to engage a high level processing devoted to detect, on pixel basis, semantic regions related to a few classes having the most perceptive impact on the human visual system ([Lee et al, 1998], [Yendrikhovskij et al, 1998]): skin, vegetation, blue sky and sea. The overall results can be effectively used to further refine demosaicing process and/or implementing on-board an image classification scheme able to properly tune successive processing steps (e.g. JPEG compression [Battiato et al, 2001]).

The proposed technique definitively improves the region classifier described in ([Naccari et al, 2004], [Naccari et al, 2005]) introducing some spatial features together with a more detailed color data analysis. The enhancement technique for unsupervised automatic color rendition of natural digital images is based on adaptive color correction properly driven by a natural region classifier pixel-based (see [Naccari et al, 2004] for major details).

Differently than in [Luo et al, 2003] where a physical model-based approach was used, our semantic extraction is mainly derived making use of a sort of "regularity" measured in the HSL and normalized-RG color spaces over a large dataset of real-scene photographic images taken by non professional. In particular, the image classes under investigation have been naturally clustered, taking into account their color distribution using a PCA-based approach. For each input image the final output is a false-color image where the semantic regions considered are properly marked, as proposed both in Dominant Color in Lab based on the Mpeg-7 guidelines [MPEG Requirement Group, 2001] and in [Luo et al, 2003]. A series of subjective experiments confirm the effectiveness of the proposed algorithm.

The paper is structured as follows. The next Section describes the overall methodology of the proposed classification strategies. Section 3 explains in detail each single processing step. Section 4 briefly summarizes the enhancement strategy whereas Section 5 reports the experimental results. A brief conclusive Section pointing to future evolutions is also included.

2 STATISTICAL ANALYSIS

The semantic extraction analyzes the input image and identifies the various classes. As previously mentioned main classes for natural scenes are: skin, vegetation, blue sky and sea. Figure 1 shows the overall pipeline of the proposed method. Initially, both color and edge analysis are performed according to some measured statistical inference on the input training set. After that, the main processing steps Automatic Semantic Extraction (ASE) and Edge Semantic Extraction (ESE) based on collected statistics and PCA are used to derive a reliable region identifier.

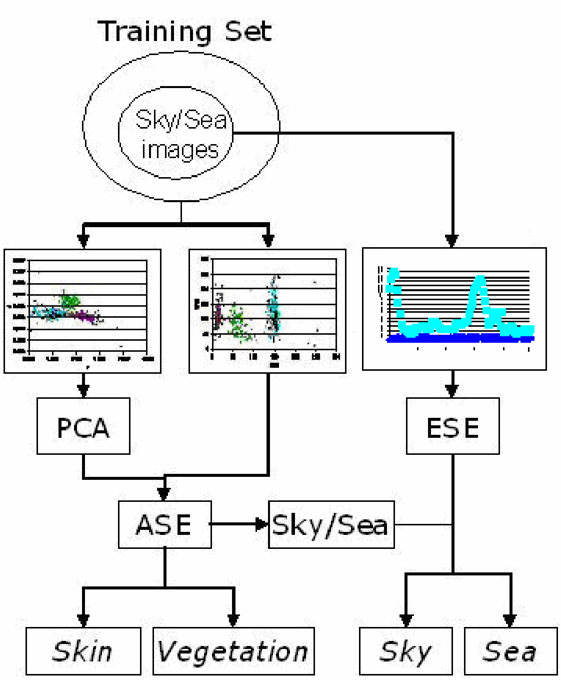

Figure 1: The pipeline of the proposed method

2.1 Macropixel Bayer to RGB Color Conversion

Acquiring images by digital CCD/CMOS sensor, in Bayer CFA format, the final chromatic components of the image have to be reconstructed by some color reconstruction technique. For our purposes, using low computational resources, an RGB images is generated converting 2x2 blocks of the input CFA data into a RGB pixel, in the following way (Figure 2). The green value is obtained as

$$G_i = \frac{G_{R_i} + G_{B_i}}{2} \tag{1}$$

where G_{Ri} and G_{Bi} are the green values in the i-th 2x2 block. The red and the blue values are simply retained. This color conversion technique leads to a RGB image with reduced dimensions respect to the original image. The chromatic information are however enough to proceed with the successive steps.

2.2 Color Statistics and Features Extraction

A large database of “high-quality” natural scene images have been used as the training set in order to characterize the chromatic properties of the color classes under investigation. All images have to be chosen according to perceived naturalness principle [Yendrikhovskij et al, 1998]. Images affected by severe color cast and/or anomalous color distortions (according to a common sense of expected color/scene pairing) have not been considered. To avoid collecting statistics on excessively scattered color samples, we used an automatic segmentation algorithm [Comaniciu et al, 1997] to initially extract homogeneous chromatic regions related to the basic color classes. Collected statistics show that the HSL and normalized-RG color space mapping are well suited for reliable chromatic classification (Figure 3). The “luminance” channel in HSL color space is not used to have a “luminance independence” strategy. The training set has been used to properly derive the corresponding parameters devoted to discriminate between the various classes. As can be noted in Figure 3, the input data can be clustered according to the vertical clustering depicted in Figure 3a and the ellipses in Figure 3b. Following this strategy a simple punctual *H-rg* based selection can be performed over the pixels in order to establish the belonging to the chromatic classes under detection. While vertical threshold can be manually tuned, ellipses parameters require a computation performed using the PCA as explained later. A “draft” region identifier is then obtained although it is not yet capable to discriminate between sky and sea. These two classes cannot be discriminated by simply using color information: a deeper strategy is definitively needed.

The principal component analysis (PCA) is a standard technique to remap a dataset defined over a vector space into another one in which meaningful components are aligned to the vector basis. PCA is typically used to reduce the overall number of components. In our case we use PCA for a different purpose: we remap the normalized-RG color space dataset (see Figure 3b) to infer the canonical equation of the best fitting ellipse. Once these ellipses are obtained, normalized-RG color space is divided into four regions (skin, vegetation, sky/sea and other) that can be directly used for region identification.

The sea is often indistinguishable from the sky [Luo et al, 2003], but other information can be used to properly discriminate between them. Clearly, if a correct image orientation is known, the knowledge of possible spatial configurations could be utilized to resolve the ambiguities between sky and sea bodies. A different approach has been used here, taking into account the different magnitude of the high frequency content of the two classes as shown in Figure 3c. Using some heuristic analysis, edge detection rules have been added to reinforce classification relying on pure chromatic principles. The learning phase has used a subset of the original training set containing sky and sea (the sky/sea training set) to properly characterize and tune the involved parameters.

3 SEMANTIC EXTRACTION

3.1 Automatic Semantic Extraction (ASE)

This step analyzes the input color image in order to identify regions belonging to specific, real world classes. Once such regions have been identified, a mask M, properly coding the belonging to a specific class c of each underlying pixel is pointed out. Thus, given a pixel in position k we denote with c_k the class it belongs to. In our implementation the classification is limited to the classes: skin, vegetation, sky and sea. Of course, using the same techniques, the ASE could be easily extended to accommodate an arbitrary number of classes depending on the specific environment within they are intended to be used. Indeed, it is worth noting that once an image has been properly classified, the pseudo image could be used to support several kinds of applications (e.g. color enhancement [Battiato et al, 2004], [Naccari et al, 2004] and image classification [Fredembach et al, 2004]). The image is classified on pixel basis using rules that have been easily derived from the collected statistics. In order to avoid dealing with ambiguous values coming from the saturated and/or low-lit pixels, only that ones satisfying the following condition are considered:

$$(S_k > T_S) \wedge (L_k > T_L) \qquad (2)$$

where S_k and L_k are respectively saturation and lightness values for pixel in position k, and T_S and T_L are experimentally fixed thresholds. The assignment of each pixel P_k to the available classes is handled by three mutual exclusive rules:

$$\begin{gathered}((L_c \le H_k \le R_c) \wedge ((r,g)_k \in \alpha_c)) \rightarrow P_k \in class_c \\ c \in \{skin, veg, sky/sea\}\end{gathered} \qquad (3)$$

where H_k and $(r, g)_k$ are respectively hue and rg values for pixel in position k, L_c and R_c are the hue vertical bounds for class c and α_c is the ellipse for class c. Figure 4 shows an output of our method where for sake of clarity the detected classes are identified properly choosing RGB triplets: (255,0,0) for skin, (0,255,0) for vegetation, (0,0,255) for sky/sea, coding with (0,0,0) the unclassified pixels.

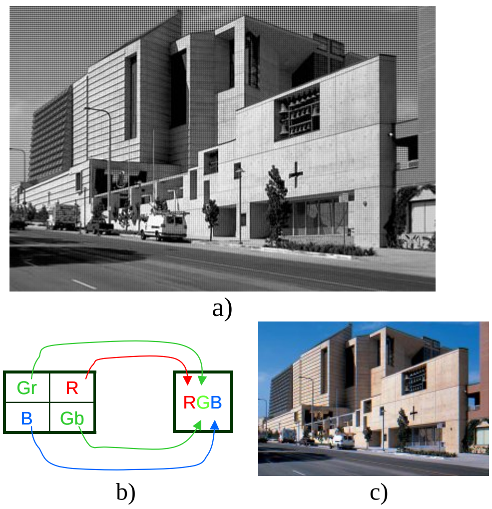

Figure 2: Bayer Pattern image a); Macropixel interpolation b); RGB image after color recovery c).

3.2 Edge Statistic Extraction (ESE)

As clearly depicted in Figure 3b some further step is needed to discriminate between sky and sea classes. The feature chosen to overcome this limitation is the edge magnitude referred to the input resolution size. Figure 3c shows the mapping obtained considering the statistic of magnitude of the sky/sea pixels, after a convolution with an edge detection kernel. The plot in Figure 3c shows how two obvious bounds to discriminate among sky, sea and unclassifiable pixels are clearly present. Two different kernels have been used: the 3x3 Laplacian filter to detect edges in low-resolution images (images lower than 2000x1500 pixels) and the 7x7 Abdou filter [Abdou et al, 1979] for high-resolution images.

Following the same above notation, the assignment of each pixel P_k to the sky or sea class is handled by two mutual exclusive rules:

$$\begin{aligned}&(D_c \le EM_k \le U_c) \rightarrow P_k \in class_c \\ &c \in \{sky, sea\}\end{aligned} \tag{4}$$

where EM_k is the edge magnitude for pixel in position k, D_c and U_c are the edge magnitude horizontal bounds for class c. Figure 3c shows how this simple heuristic rule is able to improve the discrimination power of the method.

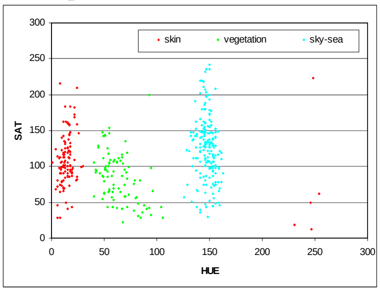

a)

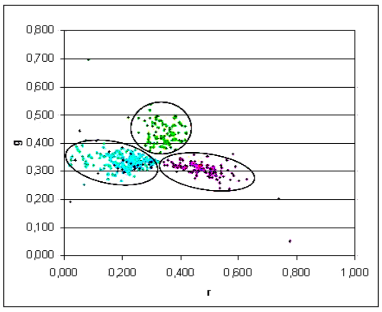

b)

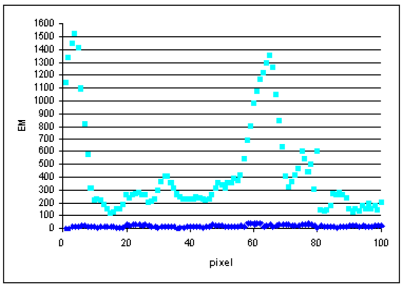

c)

Figure 3: Natural images database mapping in HS plane a), normalized-RG plane b), and Edge Magnitude plane c). Vertical H clusters in a) and ellipses in b) identify the investigated chromatic classes. Horizontal clusters in c) discriminate between sky and sea.

4 ENHANCEMENT STRATEGY

The overall enhancement strategy ([Naccari et al, 2004], [Naccari et al, 2005]) requires to properly filter the mask of each class by using a standard low pass Gaussian kernel. The filtering is performed on a down-sampled mask image followed by successive up sampling by means of bilinear interpolation. The sampling ratio and the kernel size where chosen to be proportional to input image resolution. The final mask $M = \{c_k, w_k\}$, indicating for each pixel in position k the class c_k to which it belongs, and the degree of membership w_k. Since the filtering step will cause the results of the punctual classification to overlap (e.g. multiple assignments will be available for the same pixel), a max rule is used to obtain one class and one degree of membership for each pixel.

$$\begin{aligned}&c_k = \{class_c : c = \max(w\_skin_k, w\_veg_k, w\_sky_k, w\_sea_k)\} \\ &w_k = \max(w\_skin_k, w\_vegetation_k, w\_sky_k, w\_sea_k)\end{aligned} \tag{5}$$

The enhancement is aimed to reduce the distance of colors belonging to the various classes from the target values by means of proper, lightness preserving, color shifting. The mask $M = \{c_k, w_k\}$ is used to guide this process, by assigning a class related target to the classified pixels, and by modulating the amount of color correction. For each class (skin, vegetation, sky, sea) the targets were obtained by mapping the centroids of the collected statistics on the rg (RGB normalized) chromaticity plane. Given an RGB color, the mapping on the rg plane can be defined as:

$$r = \frac{R}{R+G+B}$$
$$g = \frac{G}{R+G+B} \qquad (6)$$

The computed color targets for each class c will be indicated as (r_c, g_c). After converting the input image into the rg color space employing, the mean value on the color plane of each identified color class is computed as follows:

$$\mu_{rc} = \frac{\sum_k (r_k : c_k = c)}{card_c}$$
$$\mu_{gc} = \frac{\sum_k (g_k : c_k = c)}{card_c} \qquad (7)$$

with $card_c$ representing the cardinality of class c. For each class, the offset from the target color is defined as:

$$\Delta_{rc} = r_c - \mu_{rc}$$
$$\Delta_{gc} = g_c - \mu_{gc} \qquad (8)$$

The color enhancement is carried out by shifting each pixel value (r_k, g_k) by the computed offset and then converting back in the standard RGB color space. The ambiguity, due to the "one to many" mapping, of the inverse of Eq. (6) can be advantageously used to define a lightness preserving, constrained linear system:

$$\begin{cases} \dfrac{R_k^{'}}{R_k^{'} + G_k^{'} + B_k^{'}} = r_k + \Delta_{rc} \\ \dfrac{G_k^{'}}{R_k^{'} + G_k^{'} + B_k^{'}} = g_k + \Delta_{gc} \\ \dfrac{R_k^{'} + G_k^{'} + B_k^{'}}{3} = \dfrac{R_k + G_k + B_k}{3} \end{cases} \qquad (9)$$

where (R_k, G_k, B_k) is the input color for pixel k, and (R'_k, G'_k, B'_k) its output value. In order to avoid the appearance of unpleasant artifacts and/or excessive color distortions, the final color correction is modulated by using the computed membership values w_k of the mask M, and two modifiable parameters a and b. The final values (R''_k, G''_k, B''_k) are thus defined as follows:

$$R_k^{''} = \frac{aR_k + b\left[w_k R_k^{'} + (1-w_k)R_k\right]}{a+b}$$
$$G_k^{''} = \frac{aG_k + b\left[w_k G_k^{'} + (1-w_k)G_k\right]}{a+b} \qquad (10)$$
$$B_k^{''} = \frac{aB_k + b\left[w_k B_k^{'} + (1-w_k)B_k\right]}{a+b}$$

Parameters a and b allow to perform a linear combination between original and color corrected pixel values, while weights w_k decrease or increase the amount of correction depending on the reliability of the classification. This approach allows us to preserve the dynamic range of the classified regions avoiding also a naturalness modification.

5 EXPERIMENTAL RESULTS

The overall method has been tuned using as training set a large dataset of real-scene photographic images taken by non professional. As previously mentioned all images are acquired by using "high quality" settings both in terms of resolution and compression size, according to perceived naturalness principle [Yendrikhovskij et al, 1998] excluding images affected by severe color cast and/or anomalous color distortions. The training set is obtained, generating the corresponding bayer data, properly subsampling input data; the effectiveness of the method is not affected by this approximation.

The method has been implemented in ANSI C and the overall complexity could be considered negligible mainly in the detection steps; indeed it could be easily embedded in imaging devices where usually limited resources are available. To validate the proposed region detection strategy, we use a database of 1000 images acquired at different resolution size, taken also with low-cost imaging devices. In the verification step, all images have been acquired in CFA format and the analysis process is applied after color matrixing process, just before demosaicing. Just for comparison, Figure 5 shows the improvement obtained in the region extraction with respect to the results presented in [Naccari et al, 2004]. The overall quality enhancement, is clearly improved as showed in

. We remind that enhancement is aimed to reduce the distance of colors belonging to the various classes from the target values by means of proper, lightness preserving, color shifting. The mask of pseudo-color is used to guide this process, by assigning a class related target to the classified pixels, and by modulating the amount of color correction ([Naccari et al, 2004], [Naccari et al, 2005]). For sake of comparison some subjective tests were performed. A data set of 800 natural scenes, which did no belong to our statistic class sample, was used to perform visual assessment. 50 subjects, with no particular visual defects on color perception and without experience in digital image or color processing, expressed their opinion in a light control environment and on a CRT monitor with a standard sRGB profile. Two types of visual tests were performed: an overall preference and a comparative judgment between the original and a segmented images obtained using [Comaniciu et al, 1997]. Table 1 reports the overall preference when the input and the detected semantic region were simultaneously presented to the subject. This index represents the average in terms of percentage referred to the subject choices (2 - Very Accurate, 1 - Accurate, 0 - Acceptable, -1 - Inaccurate, -2 - Wrong) with respect to the final result. The proposed strategy has obtained an effective good score. Table 2 reports the comparative tests results performed by showing to each subject in random order a couple of images containing the original, the corresponding segmented one and our result. For each comparison (original vs. segmented/classified) a quality score was assigned. Also in this case the proposed enhancement has obtained effective performances. These results confirm the effective detection of semantic regions with respect to a simple segmentation.

A further example of global color enhancement is showed in Figure 7.

Table 1: The overall preference when the input and the detected semantic region were simultaneously presented to the subject.

Preference	Percentage %
Very Accurate	17
Accurate	39
Acceptable	32
Inaccurate	7
Wrong	5

Table 2: Comparative preference between our method and segmentation method.

Preference	Percentage %
Our Method	63
Segmentation Method	37

5 CONCLUSION AND FUTURE WORKS

A novel approach able to detect semantic regions, on pixel basis, relative to natural scene (vegetation, sky, sea, and skin) has been presented. The overall enhancement obtained by making use of such regions is able to reproduce the “expected color appearance”.

Future works will include the possibility to further extend the region classifier, just introducing metadata and spatial consideration. Major details, links and demo can be found at http://www.dmi.unict.it/~iplab.

REFERENCES

Abdou, I.E., Pratt, W.K., 1979. Qualitative Design and Evaluation of Enhancement/Thresholding Edge Detector, *Proceedings of IEEE*, vol. 67, No. 5, pp. 753-763.

Battiato, S., Mancuso, M., Bosco, A., Guarnera, M., 2001. Psychovisual and Statistical Optimization of Quantization Tables for DCT Compression Engines. *International Conference on Image Analysis and Processing 2001*, pp. 602-606.

Battiato, S., Bosco, A., Castorina, A., Messina, G., 2004. Automatic Image Enhancement by Content Dependent Exposure Correction. *EURASIP Journal on Applied Signal Processing*, Vol. 12, pp. 1849-1860.

Bayer, B.E, 1976. Color Imaging Array. U.S. Patent 3971065.

Bosco, A., Mancuso, M., Battiato, S., Spampinato, G., 2002. Temporal Noise Reduction of Bayer Matrixed Video Data. *International Conference on Multimedia and Expo 2002*, pp.681-684.

Comaniciu, D., Meer, D., 1997. Robust Analysis of Feature Spaces: Color Image Segmentation. *Conf. Computer Vision and Pattern Recognition*, pp. 750-755.

Fredembach, C., Schröder, M., Süsstrunk, S., 2004. Eigenregions for Image Classification. *IEEE Transactions on Pattern Analysis and Machine Intelligence (PAMI)*, Vol. 26 (12), pp. 1645-1649.

Lukac, R., Martin, K., Platanoitis, K.N., 2004. Digital Camera Zooming Based on Unified CFA image Processing Steps. *IEEE Trans. on Cons. Electronics*, Vol.50, (1), pp. 15-24.

Luo, J., Etz, S.P., 2003. A Physical Model-based Approach to Detecting Sky in Photographic Images. *IEEE Transactions on Image Processing*, Vol. 3 (11).

Lee, E.J., Ha, Y.H., 1998. Favorite Color Correction for Favorite Colors. *IEEE Trans. On Consumer Electronics*, Vol. 44 (1), pp. 10-15.

MPEG Requirements Group, 2001. Description of MPEG-7 Content Set, ISO/IEC/JTC1/SC29/WG11/N2467.

Naccari, F., Battiato, S., Bruna, A., Cariolo, S., Castorina, A., 2004. Natural Scenes Enhancement by Adaptive Color Correction. *IEEE ISCE International Symposium on Consumer Electronic*, pp. 320-323.

Naccari, F., Battiato, S., Bruna, A., Capra, A., Castorina, A., 2005. Natural Scene Classification for Color Enhancement. *IEEE Trans. on Cons. Electronics*, Vol. 5 (1), pp.234-239.

Yendrikhovskij, S.N., Blommaert, F.J.J , De Ridder, H., 1998. Optimizing color reproduction of natural images. *Sixth Color Imaging Conference: Color Science, Systems, and Applications*, pp. 140 145.

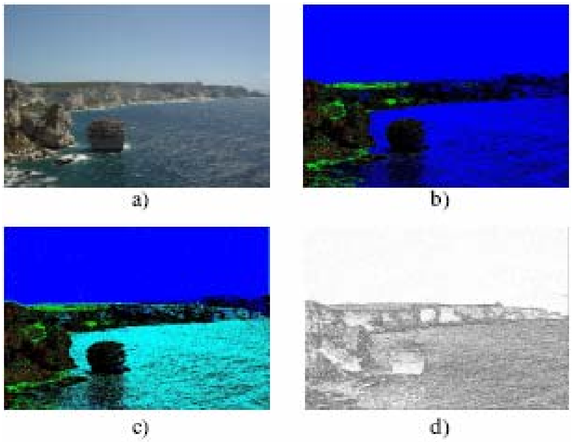

Figure 4: An example of the proposed method. a) The original image (1280 x960 pixels), b) the detection using ASE, c) the detection using ASE+ESE, d) the detected edges.

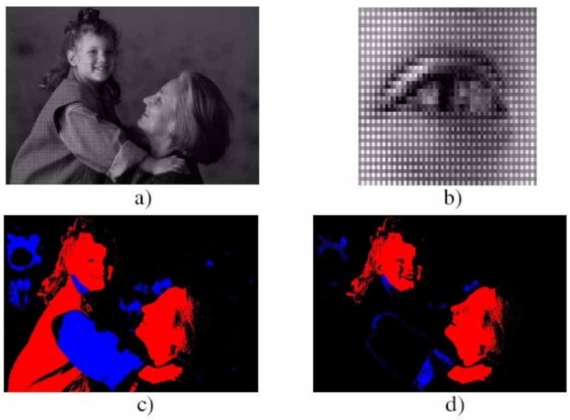

Figure 5: Examples of visual comparison between semantic regions detection applied on an input image a), obtained with our method d) and using the technique described in [Naccari et al, 2005] c). The blue and red areas of the dress in c) are now almost discarded. In b) a magnified detail of the input image showing the typical Bayer pattern.

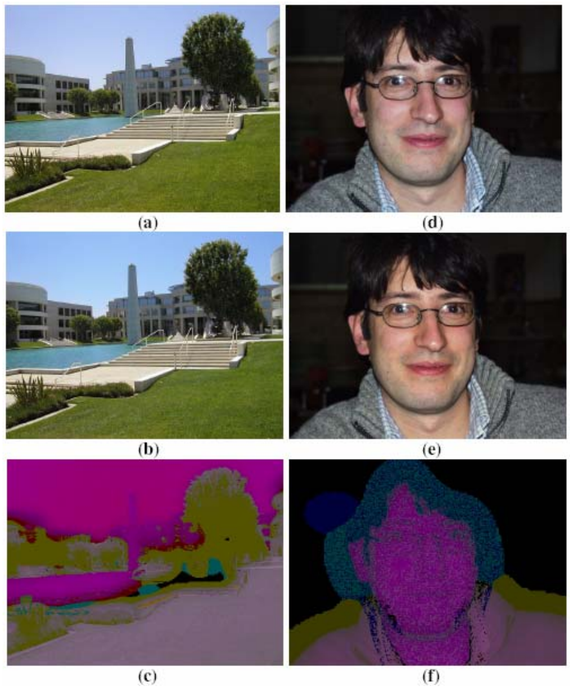

Figure 6: A landscape image (a), its enhanced version (b) and the difference image (c). A portrait image (d) its enhanced version (e) and the difference image (f).

a)

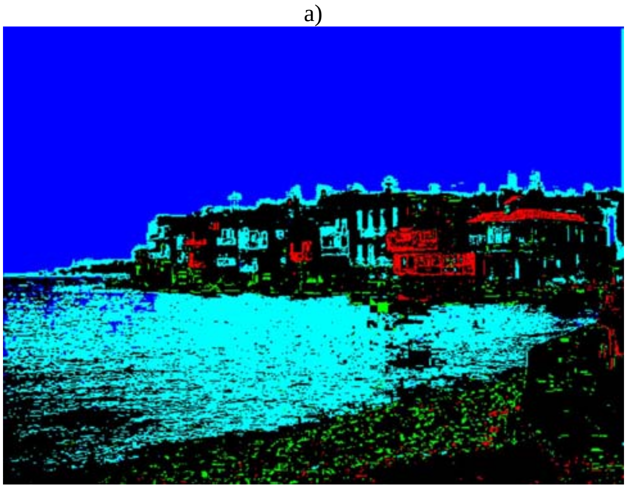

b)

c)

Figure 7 – The input image a) and its enhanced version c). The mask obtained by the proposed system b).